23PM2A-01

Electromagnetics of Active Coated Nano-Particles

Samel Arslanagić

Department of Electrical Engineering, Technical University of Denmark
Ørsteds Plads, Bldg. 348, DK-2800 Kgs. Lyngby, Denmark
sar@elektro.dtu.dk

***Abstract*—This work reviews the fundamental properties of several spherical and cylindrical active coated nano-particles excited by their respective single and/or multiple sources of radiation at optical frequencies. Particular attention is devoted to the influence of the source location and orientation, the optical gain constant and the nano-particle material composition on the electric and magnetic near fields, the power flow density, the radiated power as well as the directivities. Resonant as well as quasi-transparent states will be emphasized in the discussion.**

I. Introduction

It is known that including plasmonic materials (like silver, gold, or copper) to achieve a negative permittivity in the cylindrical or spherical shell of a coated nano-particle (CNP) can lead to novel optical properties such as resonant scattering and transparency and thus to features that may be useful for, e.g., nano-sensor technologies [1]-[3], optical invisibility [4]-[7], and nano-antennas [8], [9]. Despite the great potential of plasmonic materials and CNPs, their use in applications is, however, limited by the large absorption losses at optical frequencies. However, as demonstrated in [10], for a spherical CNP, these losses can be overcome by including gain in the system, leading to novel optical properties in the scattering and absorption cross-sections of these active CNPs. In particular, a "super" resonance was identified with a scattering cross-section substantially greater than that of a tuned, resonant passive CNP, thus making the active CNP a favourable candidate for sensor and antenna applications with significantly increased sensitivities and near-field enhancements. In many cases, the CNPs were of a spherical shape (either a single plasmonic sphere, or a core-sphere layered by a concentric shell where both dielectrics and plasmonics were used) and the source of excitation was taken to be a plane wave.

In recent works [11]-[17], electromagnetic properties of canonically shaped CNPs (cylindrical and spherical) were examined in the presence of more realistic sources of radiation such as electric Hertzian dipoles and electric, as well as magnetic, line sources. It was shown that appropriate gain inclusion in such configurations may lead to super-resonant states with profound localization of electromagnetic fields and power density inside the CNPs, as well as to enhancements and reductions of the power radiated by the respective sources. These are all features highly desirable for e.g., efficient fluorescent sensors and antennas with properties significantly surpassing those of their passive-based counterparts.

The purpose of the present work is to review some fundamental electromagnetic properties of cylindrical and spherical active CNPs as discussed in [11]-[17]. The CNPs will be excited by their respective sources of radiation. In the cylindrical case, the source is a magnetic line current, while in the spherical case, the source is one or several tangential and/or radial electric Hertzian dipoles. In all considered cases, the active CNPs are made of a canonical gain-impregnated silica nano-core covered concentrically with a silver, gold, or copper nano-shell. Particular attention is devoted to the influence of the source location and orientation, the optical gain constant and the nano-particle material composition on the electric and magnetic near fields, the power flow density, the radiated power as well as the resulting directivities. Resonant as well as quasi-transparent states will be emphasized as will be their relevance for applications.

II. Configurations, Results and Discussion

The configurations of spherical and cylindrical CNPs reviewed inhere are shown in Fig. 1. In both cases, they consist of a dielectric nano-core (green region) which is covered concentrically by a plasmonic nano-shell (red region); in the cylindrical case, the configuration is infinite in the *z*-direction. The cylindrical CNP is excited by an arbitrarily located magnetic line source (MLS) which is parallel to the axis of the cylinders, while the spherical CNP is excited by an arbitrarily located and oriented electric Hertzian dipole (EHD). The analytical electromagnetic field solutions for the CNPs in Fig. 1 have been derived in [11, Ref. 23] and [13, Ref. 8], and were used in [11]-[17] to study their fundamental properties in terms of electric and magnetic near-field distributions, power flow density, radiated power, and directivity.

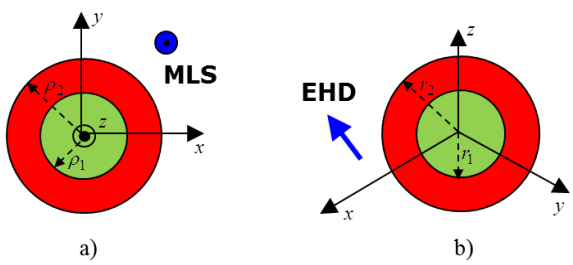

Fig. 1. Cylindrical a) and spherical b) CNP configurations.

In [11]-[17], significant attention was devoted to a CNP made of a *silica (SiO_2) nano-core* of radius 24 nm, coated with a 6nm thick *silver (Ag), gold (Au), and/or copper (Cu) nano-*

shell for which the size-dependency of the permittivity was taken into account [10]; these will be the ones reviewed in here. For the active CNP, the constant frequency gain model, where gain is added to the lossless silica nano-core, was considered. Thus, the nano-core permittivity takes on the form $\varepsilon_1 = (n^2 - \kappa^2 - 2jn\kappa)\varepsilon_0$,where $n = \sqrt{2.05}$ is the refractive index of the silica nano-core in the frequency region of interest, and the parameter κ determines the nature of the nano-core and thus of the CNP; it becomes lossless (and passive) for $\kappa = 0$, lossy and passive for $\kappa > 0$ and active for $\kappa < 0$ (in which case κ is the optical gain constant [10]).

A. Cylindrical Active Coated Nano-Particles

The below results represent a brief summary of [13], [15] and [16] where the properties of cylindrical active CNPs were thoroughly accounted for.

Fig. 2a) shows the so-called normalized radiation resistance (NRR) (the radiated power of the MLS in the presence of the CNP relative to the power radiated by the MLS alone in free-space) as a function of the wavelength, λ , for Ag-, Au, and Cu-based CNPs with a) $\kappa = 0$ and b) the values of κ that result in very large radiated powers, this corresponding to the so-called super-resonant states. The MLS current is 1 V/m and is placed inside the nano-core at 12 nm on the positive *x*-axis. While the response of the passive CNPs is found to be dominated by the large absorption losses and thus low NRR values, the plasmonic material losses are overcome by gain inclusion, thus leading to significantly increased NRR values. The values of κ , the NRR, and the wavelength λ for the super-resonant states in Fig. 1b) are, respectively, (-0.175, 51 dB, 577.7nm; Ag-based CNP), (-0.262, 56 dB, 669.4 nm; Au-based CNP), and (-0.310, 46 dB, 662.2 nm; Cu-based CNP).

The super-resonant behaviour in Fig. 1b) is not restricted to the MLS locations within the nano-core. As shown in Fig. 1c), where the NRR is shown as a function of the MLS location (along the positive *x*-axis) for the three super-resonant CNPs, particularly large NRR values result for MLS locations near the surfaces of the nano-shell, while no enhancements occur for locations at and close to the origin.

The super-resonance in the active CNPs is due to a strong excitation of the resonant dipole mode inside the CNPs. Its existence is a result of juxtaposition of two materials (one with positive permittivity (silica nano-core) and the other with negative permittivity (plasmonic nano-shell)) and whose strong excitation is heavily assisted by the gain inclusion inside the CNP. The super-resonant state of the active Ag-based CNP is further illustrated in Fig. 3a) where the magnitude (colour) and direction (arrows) of the resulting Poynting vector (power flow density) is shown for a MLS located at 12 nm along the positive *x*-axis. A very strong dipolar pattern is observed in Fig. 3a), while no resonant dipole mode is in evidence for the corresponding passive CNP, cf., Fig. 3b), this being in line with the low NRR values reported in Fig. 1a). Similar results as the one in Fig. 3b) are obtained for super-resonant Au- and Cu-based CNPs.

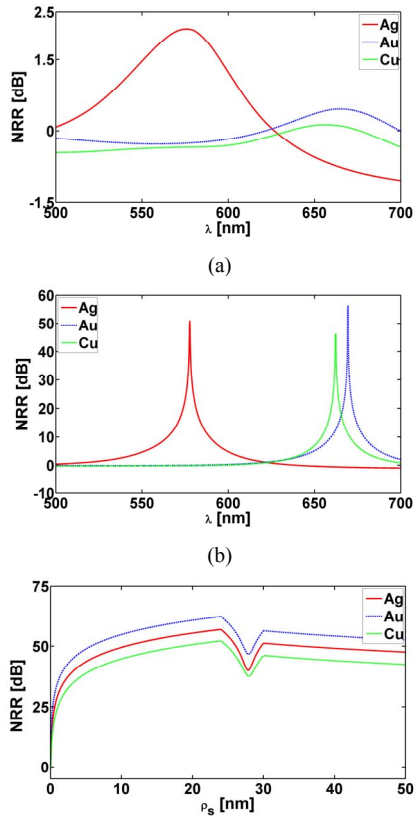

Fig. 2. The NRR as a function of the wavelength, λ, for a) lossless and b) super-resonant Ag-, Au-, and Cu-based cylindrical CNPs. c) The NRR as a function of the MLS location (along the positive *x*-axis) for the super-resonant CNPs.

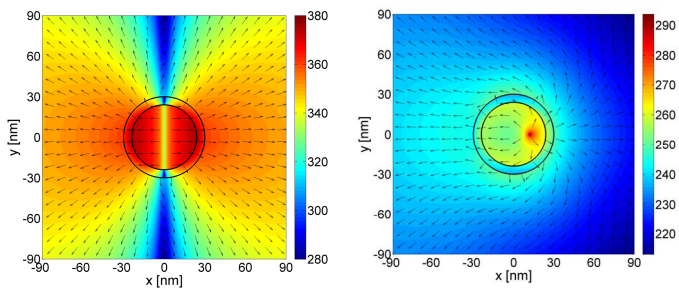

Fig. 3. The magnitude and the direction of the power flow density for the super-resonant active Ag-based cylindrical CNP (a) and for the corresponding passive Ag-based CNP (b). The MLS is located at 12 nm along the positive *x*-axis. Note that the dynamic range in (a) is larger than that in (b). The curves representing the cylindrical surfaces of the CNP are included in the figure.

The large variations of the NRR with the MLS location, see Fig. 2c), lead to interesting directivity pattern re-shaping possibilities for the super-resonant CNPs [15]. Apart from these, the work in [15] also revealed that for a fixed source location, the directivity can be re-shaped by adjusting the optical gain constant. The influence of both mechanisms on the directivity patterns will be discussed in the presentation.

B. Spherical Active Coated Nano-Particles

The below results represent a brief summary of [11], [12], [14], [15], and [17], where the properties of spherical active CNPs were thoroughly accounted for. In the present discussion we consider both an *x*- and a *z*-oriented EHD with their dipole moments set to 5E-09 Am.

1) Single-Source Excitation: Fig. 4) shows the NRR as a function of the wavelength, λ, for the Ag-based CNP for (a) $\kappa = 0$ and (b) $\kappa = -0.245$, where the latter corresponds to the optical gain constant leading to the super-resonant states, and thus to the largest NRR (of about 72.5 dB at 502.1 nm) for both EHD orientations (the respective EHDs are located inside the nano-core at 12 nm along the positive *x*-axis). The results in Fig. 4 thus clearly show that the gain inclusion inside the spherical CNPs vastly overcomes the intrinsic plasmonic losses, thereby leading to significantly increased NRR values relative to the case of the corresponding passive Ag-based CNP for which largest NRR is around 17 dB (at 502.7 nm. Although not shown in here, the values of κ, the NRR, and the wavelength, λ, for the super-resonant states are, respectively, -0.532, 74 dB, 597.4 nm, for the Au-based CNP, and -0.741, 68 dB, 601.7 nm, for the Cu-based CNP.

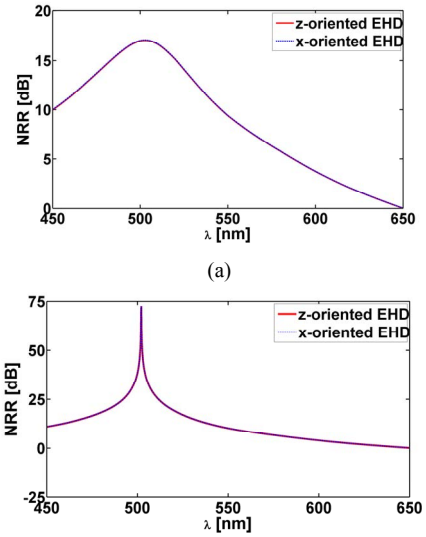

Fig. 4.The NRR as a function of the wavelength, λ, for the spherical Ag-based passive (a) and super-resonant (b) CNP. The results are shown for both *z*- and *x*-oriented EHDs, and in all cases the EHD is located in the silica nano-core at 12 nm along the positive *x*-axis.

As in the cylindrical case, the super-resonances reported in Fig. 4b) are due to a strong resonant dipolar mode that is excited inside the CNPs. This is illustrated in Fig. 5 where the magnitude of the θ-component of the electric field is shown for the Ag-based CNP with $\kappa = -0.245$ and $\lambda = 502.1$ nm for the *z*-oriented EHD (Fig. 5a), and for the *x*-oriented EHD (Fig. 5b)). The excited modes correspond to those of a *z*- and *x*-oriented EHD, respectively, located at the origin, and they are both very strongly excited with comparable magnitudes.

We moreover note that the super-resonance phenomenon in Fig. 4b) and Fig. 5 is not restricted for the EHD locations inside the nano-core of the CNP. As shown in Fig. 6, large NRR values are also obtained for the EHD locations inside the nano-shell and outside the CNP.

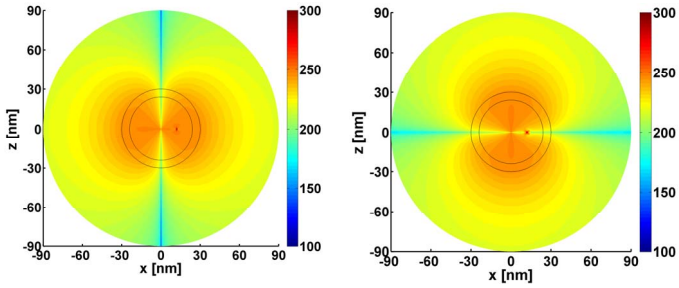

(a) (b)

Fig. 5. The magnitude of the θ-component of the electric field of the super-resonant spherical Ag-based CNP for (a) *z*-oriented EHD and (b) *x*-oriented EHD. The EHD is inside the nano-core at 12 nm along the positive *x*-axis.The observation plane is the *xz*-plane. The curves representing the spherical surfaces of the CNP are likewise shown in the figure.

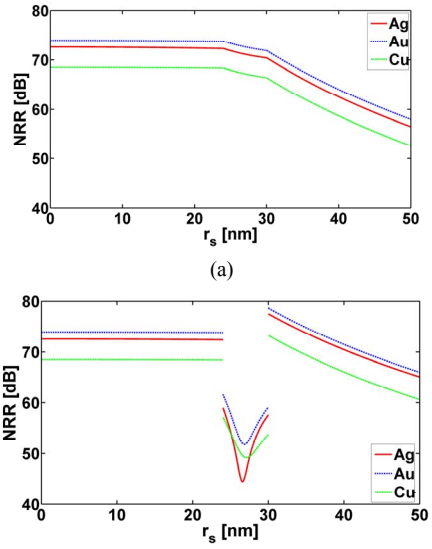

Fig.6. The NRR as a function of the EHD location along the positive *x*-axis for the spherical super-resonant Ag-, Au-, and Cu-based CNPs. (a) *z*-oriented EHD and (b) *x*-oriented EHD.

Comparing the results for the two EHD orientations in Fig. 6, two notable differences are observed. First, the NRR of the *x*-oriented EHD is well below that of the *z*-oriented EHD when the EHDs are inside the respective nano-shells. For the *x*-oriented EHD, some of its field gets trapped inside the nano-shell (i.e., the nano-shell acts as a waveguide excited by the EHD oriented orthogonal to its walls), and thus does not get radiated, resulting in reduced NRR values. The second notable difference between the two orientations occurs for the EHD locations outside the CNPs. For these locations, the NRR for the *z*-oriented EHD drops below its values obtained when the EHD is inside the CNPs, while the NRR for the *x*-oriented EHD attains its maximum as the *x*-oriented EHD moves just outside the CNP; this maximum is also larger than any of the

NRR values obtained with the *z*-oriented EHD. The *x*-oriented dipole not only excites the resonant mode of the electrically small core-shell cavity, but it also directly drives the surface plasmon polaritons on the outer shell, and this explains the increased NRR values for the *x*-oriented EHD outside the CNP. In summary, the strongest excitation of the resonant dipole mode requires the *z*-oriented EHD to be inside the nano-cores, while the locations of the strongest excitations for the *x*-oriented EHD are those just outside the CNPs.

2) Multiple-Source Excitation: While the super-resonant CNPs discussed above support the excitation of the super-resonant states, it is very interesting to note that they also can be used to decrease significantly the radiated power (in the far-field region) of the EHD when it is located outside the CNP. For a single *z*-oriented EHD (EHD A) located outside the super-resonant Ag-based CNP at 40 nm on the positive *x*-axis, Fig. 7 shows a peak in the NRR at 502.1 nm but also a "dip" in the NRR (down to -12.7 dB) at 594.9 nm.

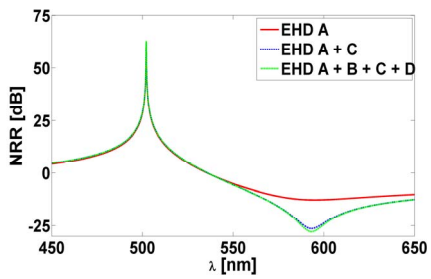

Fig. 7. The NRR as a function of the wavelength, λ, for the super-resonant spherical Ag-based CNP excited by one (EHD A), two (EHD A+C) and four (EHD A+B+C+D) *z*-oriented EHDs. See the main text for further explanations.

At this dip, the power radiated by the EHD A is effectively 12.7 dB below the value when the EHD A is radiating alone in free space. If an identical dipole (EHD C), located at 40 nm on the negative *x*-axis, illuminates the CNP simultaneously with EHD A, the dip for the NRR is significantly lowered (down to -26.4 dB) relative to the single dipole case. This additional lowering of the NRR indicates that the active CNP jams the signal of the two EHDs, effectively cloaking them to a far-field observer. Adding an additional set of dipoles, EHDs B and D, located at 40 nm at the positive and negative *y*-axis, respectively, only lowers the dip in the NRR by an additional 1.3 dB relative to the two dipole case. These interesting results will be further addressed at the presentation in terms of power flow distributions inside and outside the CNP.

III. Conclusion

Active CNP are found to overcome the intrinsic absorption losses in the constituent plasmonic materials, thereby leading to significantly enhanced values of the radiated power for both spherical and cylindrical geometries. For the spherical CNP, source locations can be found for which the active CNPs moreover leads to significant lowering of the radiated power, effectively jamming or cloaking the surrounding dipoles to a far-field observer. Both of these interesting properties can be exploited in e.g., nano-sensor applications: the super-resonance may be used for proper detection of specific emission lines, while the jamming/cloaking property may be of great potential interest in suppressing the emission lines of certain molecules, while enhancing those of others.

References

[1] D.-S. Wang, M. Kerker, and H. W. Chew, "Raman and fluorescent scattering by molecules embedded in dielectric spheroids," *Appl. Opt.*, vol. 19, pp. 2315-2328, July, 1980.

[2] J. A. Gordon, and R. W. Ziolkowski, "Investigating functionalized active coated nano-particles for use in nano-sensing applications," *Opt. Express*, vol. 15, pp. 12562-12582, Oct. 2007.

[3] N. J. Halas, "Plasmonics: An emerging field fostered by Nano Letters," *Nano. Lett.*, vol. 10, pp.3816-3822, Sep. 2010.

[4] N. G. Alexopoulos, and N. K. Uzungolu, "Electromagnetic scattering from active objects: invisible scatterers," *Appl. Opt.*, vol. 17, pp. 235-232, 1978.

[5] J. B. Pendry, D. Schurig, and D. Smith, "Controlling electromagnetic fields," *Science*, 312, 1780, 2006.

[6] G. W. Milton and N.-A. P. Nicorovici, "On the cloaking effects associated with anomalous localized resonance," *Proc. R. Soc. A*, vol. 462, pp. 3027-3059, Mar. 2006.

[7] A. Alú, and N. Engheta, "Plasmonic and metamaterial cloaking: physical mechanisms and potentials," *J. Opt. A: Pure Appl. Opt.*, vol. 10, 2008, doi: 10.1088/1464-4258/10/9/093002.

[8] A. Alú, and N. Engheta, "Enhanced directivity from subwavelength infrared/optical nano-antennas loaded with plasmonic materials or metamaterials," *IEEE Trans. Antennas Propagat.*, vol. 55, pp.3027-3039, Nov. 2007.

[9] P. Bharadwaj, B. Deutsch, and L. Novotny, "Optical antennas", *Adv. Opt. Photon.*, vol. 1, no. 3, pp. 438–483, 2009.

[10] J. A. Gordon and R. W. Ziolkowski, "The design and simulated performance of a coated nano-particle laser," *Opt. Express*, vol. 15, pp. 2622-2653, Mar. 2007.

[11] S. Arslanagić and R. W. Ziolkowski, "Active coated nano-particle excited by an arbitrarily located electric Hertzian dipole - resonance and transparency effects," *J. Opt. A*, vol. 12, 024014, Feb. 2010.

[12] S. Arslanagić and R. W. Ziolkowski, "Active coated nano-particles: Impact of plasmonic material choice," *Appl. Phys. A*, vol. 103, pp. 795-798, Jun. 2011.

[13] S. Arslanagić, Y. Liu, R. Malureanu, and R. W. Ziolkowski S. Arslanagić, and R. W. Ziolkowski, "Impact of the excitation source and plasmonic material on cylindrical active coated nano-particles," *Sensors*, Vol. 11, 9109-9120, 2011.

[14] R. W. Ziolkowski, S. Arslanagić, and J. Geng, "Where high-frequency engineering advances optics: active nanoparticles as nanoantennas," to appear in *Optical Nanoantennas*, Eds. A. Alú and M. Agio, Cambridge University Press, London, 2013.

[15] S. Arslanagić and R. W. Ziolkowski, "Directive properties of active coated nano-particles," *Advanced Electromagnetics*, vol. 1, No. 1, May, 2012.

[16] S. Arslanagić, "Power flow in the interior and exterior of cylindrical coated nano-particles," *Appl. Phys. A*, Nov. 2012, Doi: 10.1007/s00339 -012-7380-x.

[17] S. Arslanagić and R. W. Ziolkowski, "Coated nano-particle jamming of quantum emitter," AP-S/USNC-URSI Symposium, July 08-14, 2012, Chicago, IL, USA.